Reconstruction of the waterways connections in the Danube delta since the Antiquity until the Middle Age

Final scientific report

The aim of this research project was to build the scenarios of deltaic landscape evolution in order to track the navigable routes at different historical moments. To get further insight into the deltaic dynamics during the mid and late Holocene, our research includes geomorphological, geochemical, and biological (paleovegetation, paleofauna) data, at one hand and historical and archaeological sources on the other. Further is detailed the research material and methods and the results.

Each series of data was analysed according to the methodology of its discipline. Four new sedimentological cores (Sir 1, Par 1, Par 2 and Kil1 of 8 m, 10 m, 4.5 m and 4 m respectively) were retrieved with Eijkelkamp Cobra TT percussion corer system which were topographically positioned using Leika DGPS. Additionally, geochemical, paleofauna and paleovegetation, microand microcharcoal analyses have been undertaken on KIL_1 and paleofauna and microcharcoal inventory on PAR_2.

The cores sampled in PVC tubes (ø 5cm) were cut in halves, cleared with glass knife and covered with thin plastic for Magnetic Susceptibility (MS) determinations with Bartington MS 2 susceptibility reader every 2 cm.

Sediment texture analysis

Sediment samples for grain-size analysis were taken every 5-10 cm depending on sediment texture changes. After the organic matter removal with acetic acid (30%) and hydrogen peroxide (10%) the samples were washed with distilled water and treated with 1% sodium polyphosphate solution to prevent fine particle flocculation. The grain size was measured with a Laser Diffraction Particle Size Analyzer LA-960 – HORIBA. In the end, grain size was calculate according to Folk and Ward (1957) classification, using GRADISTAT software 8.0.

Loss of ignition (LOI)

For this type of analysis the samples were dryed for 24 hours at a room temperature. About 3 g of sediment were placed in the oven (Caloris L 1003), and burned in three successive steps: at 105°C for 24h; at 550°C for 6h and at 950°C for 2h. After each burning the samples were weighed with an accuracy of 10⁻⁴g. Finally, we calculated the percentage of organic matter and inorganic carbon for each sample, by applying Heiri's (2001) formulas.

Elemental determinations were performed by means of Energy Dispersive X-ray Fluorescence (ED-XRF) to get insight into the mineralogic composition of the sediments. The analyses were performed using a portable Bruker Tracer S1 Titan spectrometer. This spectrometer uses a Rhodium (Rh) anode tube to generate an X-ray beam to probe the samples. The generated beam has a maximum energy limited at 40 keV. The beam is passed through a collimator, resulting in a spot with 8 mm in diameter on the selected samples. A Silicon Drift Detector (SDD) positioned backwards at an angle of approximatively 45° with respect to the Rh-anode tube, was used to record the spectra. One point randomly selected was analysed on each sample, each point was exposed to the beam for 60 s. Each characteristic spectra was later analysed in order to obtain elemental concentrations. The results obtained are expressed in parts-per-million (ppm).

To minimize the errors associated to grain size geochemical elements dependency, up to 10 g of material from each depth was collected and reduced mechanically. The material was homogenized and an aliquot of 2g was compressed into a pellet using a 25 tons automated hydraulic press (Specac). The resulting pellets were placed into a plastic holder until the analysis.

Paleovegetation analysis

Sediment preparation included the application of the standard procedures for the extraction of pollen and microspores (Faegri and Iversen 1989). A pollen sum of ca. 300 grains including pollen of tree and herb taxa but excluding Cyperaceae, aquatic taxa and spores was used to calculate the pollen percentages. Between 140 and 200 cm depth pollen concentration was too low to be recorded. For calculation and construction of the pollen diagrams, the PSIMPOLL 3.00 (Bennett 2007). Microscopic charcoal particles (> $75 \mu m^2$) were also counted in these slides, following the criteria of Clark (1988): black, completely opaque and angular.

Paleofauna inventory

The microfaunistic study was based on 22 micropaleontological samples collected from the KIL core (Fig. 1). Each sample weighed about 100g and all of them were washed and sieved through a sieve with 63 µm mesh size following a standard micropalaeontological approach (Stoica et al., 2013)

Macrocharcoal sample processing

Sample volume was determined with the volumetric (water displacement) method.

Samples (2-3cm²) were defloculated with 10% KOH overnight, sieved and then bleached for 3 hours using 3% natriumhypochlorid (NaClO), and sieved again with a mesh size of 150 um. (Feurdean et al., 2013).

Macroscopic charcoal (>150 um) determination was performed under the stereomicroscope, x 35-45 magnification, using a grid for the determination of macroscopic charcoal area. Charcoal number vs. area comparison may help the interpretation regarding the influence of taphonomic processes on charcoal deposition or biases resulting from mechanical fragmentation of charcoal during subsampling and sample preparation.

Morphological classification of charred particles (to distinguish between woody and non-woody fuel) was performed after Jensen et al. (2007), Mustaphi and Pisaric (2014) and Feurdean et al. (2017). Size-class-based classification (to identify the more local fire episodes) was performed after Florescu et al (2018). Recent studies showed that macrocharcoal >500 um reflects fires occurred very close (max. 1-2 km) to the sampling site, whilst smaller macrocharcoal particles (150-500 um) may be transported over greater distances (as far as 10 km or more; Vachula et al., 2018). The main charcoal morphotypes were classified as: i) *poaceae* including grass, but mostly reed; ii) *herbaceous material* containing mostly forbs, but there might be also unidentifiable grass fragments; iii) *leaves* as the particles having a typical leaf morphology; they are mostly forb leaf fragments, but some might also be grass leaf fragments; iv) *wood* identified by the presence of bordering pits, ray cells and other morphological characteristics of wood.

Absolute dating

Radiocarbon dating by accelerator mass spectrometry (AMS was conducted at Ro-AMS laboratory at Horia Hulubei National Institute for Physics and Nuclear Energy.

The samples containing organic materials and shells were pretreated according to (Sava et al., 2019). Conventional radiocarbon ages were normalized relative to the international standard (NIST SRM 4990C) Oxalic Acid II, so that 74,59% of the activity represents the reference of the modern 14 C activity. Measured radiocarbon ages were corrected for blank level and isotopic fractionation using δ^{13} C, which was calculated against VPDB standard material. The ages were finally calibrated using OxCal online V 4.4 (Ramsey, 1995) and IntCal13 atmospheric curve (Reimer et al., 2013). The chronological references are expressed as years BP (1950) together with the calibrated age intervals for the ages obtained by radiocarbon dating (Table 1)

Archaeological traces

The archaeological finds are rare and problematic in the northern delta. East of Tulcea (ancient *Aegyssus*), all settlements older than 500 years seem to have been located on the mainland in the historical region of Bassarabia (Ukraine). One archaeological excavation was undertaken in Romania (Old Chilia); further surveys and rescue campaigns brought no conclusive results. Besides the Bronze Age tumuli with secondary inhumations (Vasiliu, 1995; Mănucu-Adameșteanu, 1989), fragments of shipwrecks, scattered coins and sherds have been reported on the Tătaru and Chilia channels, on the Old Chilia island and Periprava ridge (Micu et al., 2016).

In Ukraine, besides the general histories of New Chilia (Iorga, 1928) and typological catalogues of finds, most of the archaeological finds were never published. Heterogeneous collections of ancient, Byzantine and medieval objects can be seen in the museums of (New) Chilia and Vîlkov and are mentioned on social networks. By examining these scattered references, we have tried to map the dynamics of the settlement pattern during the last 5000 years.

Historical texts and maps

All the ancient, medieval, and modern texts and maps known until now have been read in their original Greek, Latin, Slavonic, Italian and Ottoman manuscripts, in critical editions, compendia and atlases (like the *Atlas* 2008 and 2011), with extensive bibliography. We investigated the cultural context of creation and transmission of each document and tried to explain its place in the literary and cartographic tradition. Despite the rarity of eye witnesses, the historical evidence is extremely coherent, and the deviations (original inputs or productive errors) can be always explained, once one has identified the sites. The detailed analysis of all the spatial

representations, compared with the geoarchaeological data, allow us to propose new historical scenarios for the last six millennia.

Sediment characteristics, paleofauna and chrono-stratigraphy

The characterization of the sedimentation patterns in the northern part of the Danube delta following the emergence of the latest Danube's distributary is based on the assessment of the sediment texture (i.e. mean grain size and sorting), organic matter (OM) content: total organic content - TOC, organic carbonates - C_{org}, inorganic carbonates - C_{inorg}), magnetic susceptibility (MS) measured on four new cores: Sir 1, Par1, Par2, Kil1, corroborated with the data published as F18 core (Vespremeanu-Stroe et al, 2017) and KP1 (Filip and Giosan, 2014).

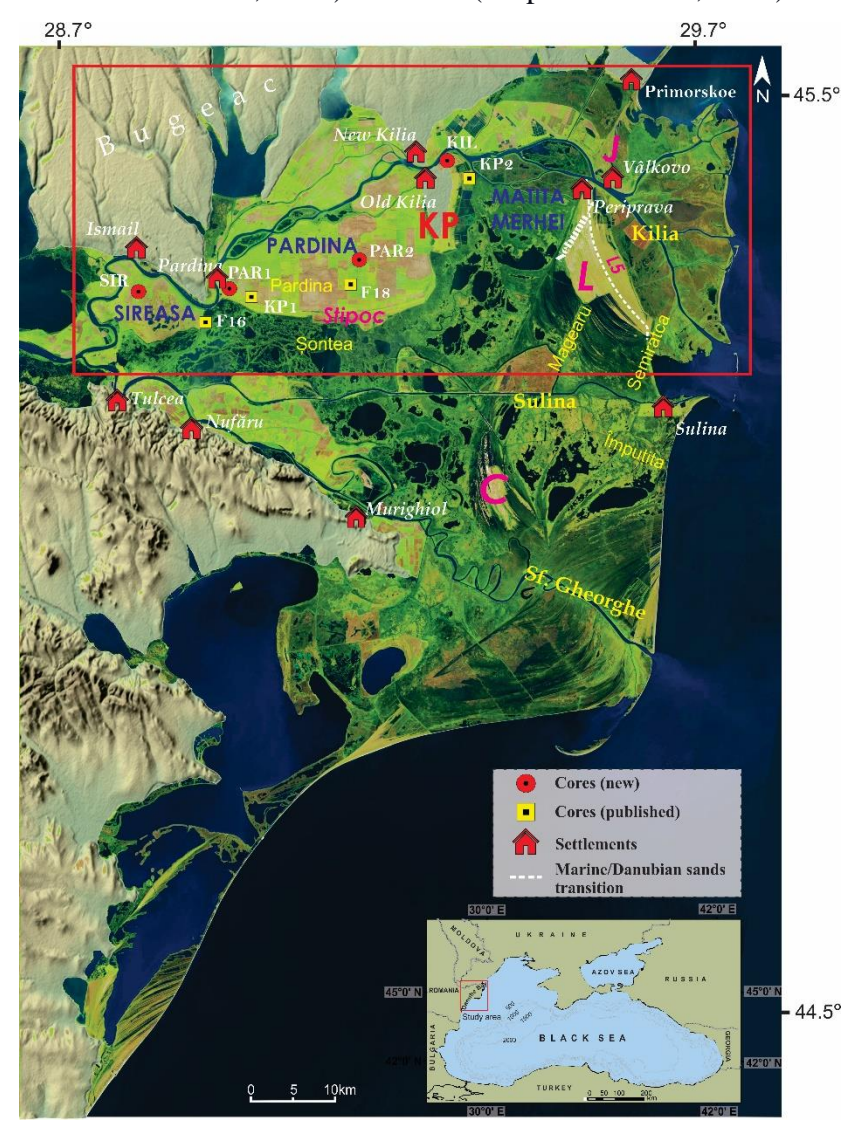


Figure 1 Sediement cores position in the Danube delta

Before entering the Pardina basin and building the first confined deltaic lobe, the Chilia distributary passed through the Sireasa basin and covered it with a thin veneer of sediments just after its diffluence from the main Danube watercourse. The sediment characteristics of the SIR core feature the advection of predominantly coarse silt and clay particles intertwined with fine sand at the upper part of the core. The core was extracted about 2 km east of the present Chilia channel (Figure 1) with the aim to investigate deltaic stratigraphy in proximity to the bifurcation of the Danube into the Tulcea and Chilia arms. Four main depositional units can be identified here according to significant changes in the sediment texture, OM content, and MS values (Figure 2). At the lower part of the core, from 800 to 400 cm, thin veneers of sand alternate with silt (ca 1-2 cm thick). MS values are highest between these depths, reaching mean values of 3.10⁻⁵ SI with numerous large amplitudes (stdev: 1.27), which probably reflect several detritic pulses. This unit has relatively low OM values (3.2%) and is predominantly inorganic (2.3%) (Figure 2). After a 50 cm layer of bulk sand between 475 cm and 425 cm, a new sedimentation cycle begins (starting from ca. 5400 yr BP) with sediments changing to fine silt and clay between 428 and 329 cm. The distribution of OM and Cinorg shows the largest variability along the core, with four peaks disrupting the trend of the organic content at 422 cm, 399 cm, 329 cm, and 239 cm. Noteworthy, the structure of thin veneers (i.e., cm size) of fine sand or coarse silt intertwined with OM laminae reappears from 240 cm until 130 cm. An almost 100 cm layer of peaty mud was found from 120 cm to 25 cm and capped by soil. MS values are comparatively low with more constant values, whereas mean OM increases to 11.7% and C_{inorg} decreases to 0.5%.

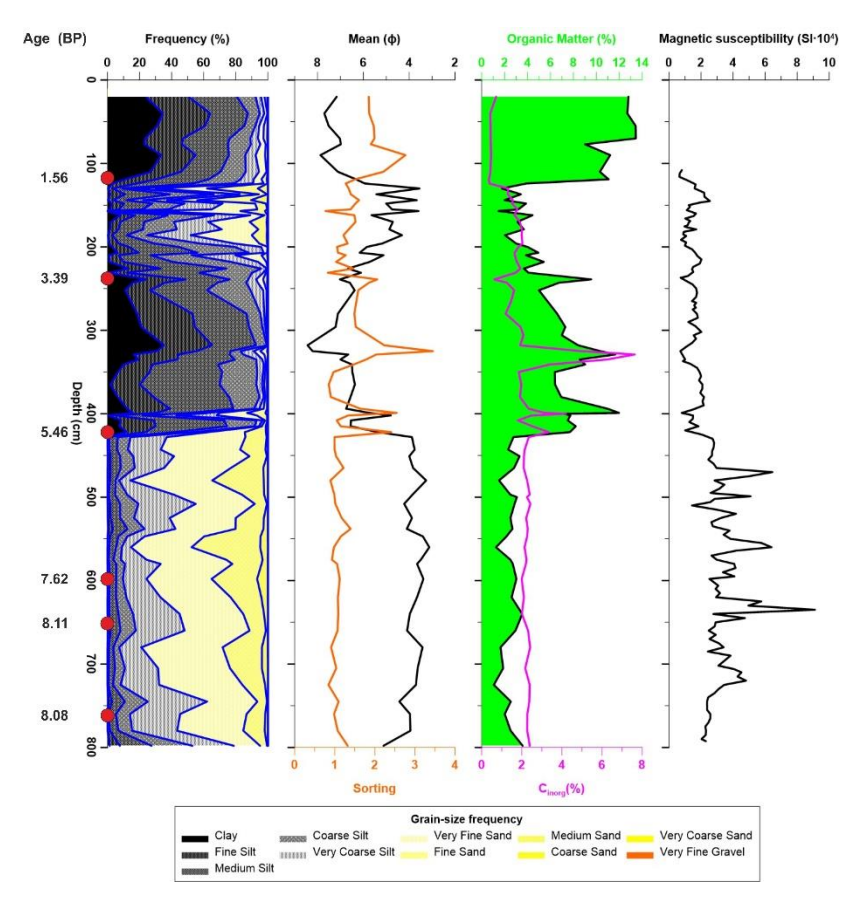


Figure 2 Grain size and sorting, organic matter content and magnetic susceptibility on Sir core The PAR 1 core was retrieved further downstream along the Chilia distributary in the southwestern part of Pardina basin (Figure 1). Four radiocarbon ages constrain the chronostratigraphy, which was cross-checked with the ages obtained by Filip and Giosan (2014) at a nearby location. The lowermost unit comprises very fine sand and coarse silt laminae at the base between 975 and 920 cm followed by homogeneous silt layers up to 775 cm (Figure 3). Mean OM (4.5%) and C_{inorg} (2%) are relatively homogeneous with high values. An upward coarsening from silt to moderately sorted very fine sand is found up to 657 cm accompanied by a rapid drop in the OM content. This sandy unit is overlaid by half a metre of coarse silt (486 to 437 cm) with large variations in the organic and inorganic carbonate content. These changing depositional conditions occurred about 4500 yr BP, as indicated by the radiocarbon age obtained at 450 cm depth (Table 1).

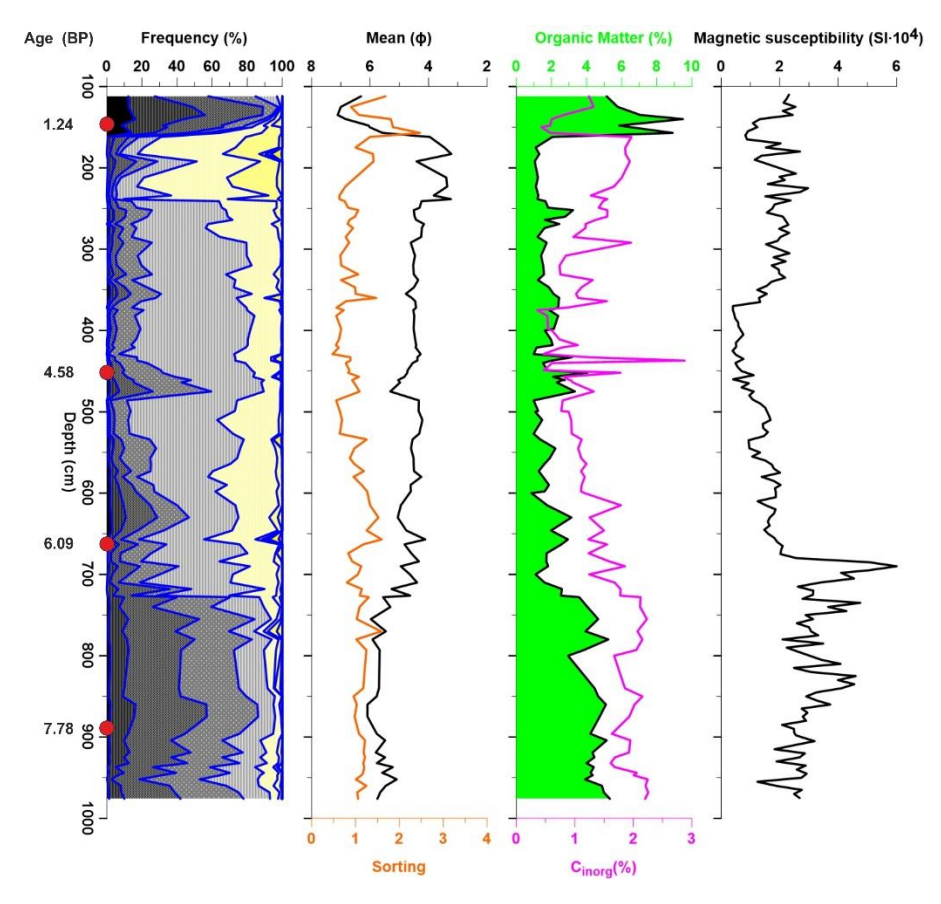


Figure 3 Grain size and sorting, organic matter content and magnetic susceptibility on Par 1 core The laminated silts at the bottom of the core accumulated within a predominantly freshwater environments which was subsequently invaded by brackish and marine fauna about 7.7 yr BP according to the radiocarbon age obtained at 900 cm. The layer from 800 cm to 750 cm is populated solely with freshwater ostracods species. Paleofauna analysis identified 7 species and 5 subspecies (Amnicythere sp.) indicative of brackish to marine environment, one marine foraminifera species (Ammonia beccarii), one euryhaline species and only 2 species of freshwater environment. This microfauna assemblage usually characterizes a brackish to marine depositional environment from 725 to 650 cm. The unit is overlaid by very coarse silt which prevails until 241 cm, excepting two peaks of coarse silt at 630 and 475 cm. The ostracods and forams populations decline both as species and specimens (one freshwater species: Dawinula stevensoni; one euryhaline species: Cyprideis torrossa; two species indicative of brackish and marine conditions: Heterocytereis, Amnicytere quinquetuberculata) from 650 cm to 540 cm reflecting a turn toward brackish to marine conditions. From 540 cm upwards the brackish and marine species disappear whereas only freshwater species increases (Darwinula stevensoni, Candona schweyeri, Candona neglecta,

Eucypris sp.) and become more abundant. The radiocarbon age obtained at 600 cm depth indicates this layer was accumulated ca. 6000 yr BP. This relatively homogenous sequence is disturbed between 486 and 437 cm by the rapid coarsening upward silt layer with large variations of the organic and inorganic carbonate content (stdev 0.44, and respectively 0.74). This changing depositional conditions occurred about 4500 yr BP as indicates the radiocarbon age obtained at 450 cm depth (Table 1). From 241 to 161cm the sedimentation consists predominantly of poorly sorted fine sands with a higher content of C_{inorg} (1.93 %) and a lower weight of organic matter (0.57%). The sediment fraction changes to medium and fine silts along with a rapid increase of the organic matter content, which reaches the highest values along the entire core (2.74%) indicating the turn to a stagnant water body which was drained in the end. The change from sand to silt deposition was dated to ca. 1200 yr BP at 150 cm.

Par 2 core is 450 cm deep, located on a levee of a former secondary channel crossing eastward Pardina lagoon (Fig.1). Four depositional sequences have been distinguished based on the variability pattern of the mean grain size, sediment sorting, MS, C_{org} and C_{inorg} respectively.

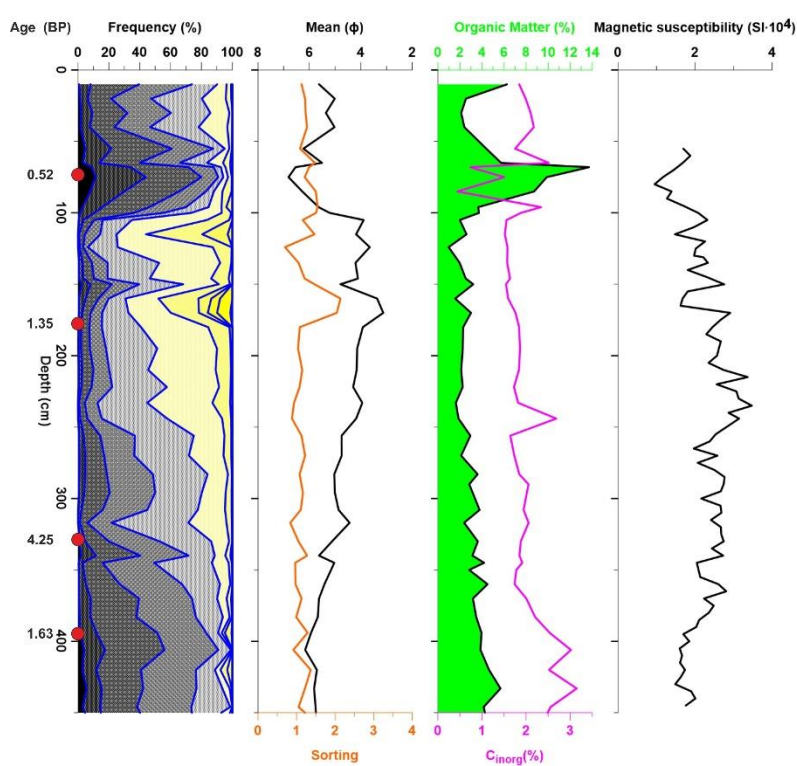


Figure 4 Grain size and sorting, organic matter content and magnetic susceptibility on Par 2 core

The PAR 2 core is 450 cm long and located on the right levee of a former secondary channel crossing the Pardina lagoon in the eastward direction (Figure 1). Four depositional sequences can be distinguished (Figure 4). Firstly, a basal layer consisting of poorly sorted coarse to medium silt from 450 cm to 370 cm was formed in Late Antiquity (1600 yr BP at 395 cm depth). This sequence is covered by very thin layers of poorly sorted coarse silt alternating with very fine sand layers until ca 200 cm. A piece of wood at a depth of 329 cm was dated to ca 4200 yr BP (Table 1), indicating the presence of reworked material. The next sediment layer up to -105 cm comprises poorly sorted very fine sand with a spike of fine sand at 170 cm. According to the radiocarbon age obtained at 175 cm, the deposition was active 1300 yr BP. The next upper layer between 105 to 65 cm is characterised by a very high OM content (6.8%) within a matrix of poorly sorted coarse and medium silt. A distinct change in the sedimentation regime occurred ca 520 yr BP when the fluvial sediment accumulation was replaced by predominantly organic deposition (peat). MS values are constant around 2 *10⁻⁵ SI, which are similar to data obtained in the upper part of the SIR and PAR 1 cores.

The 400 cm long *Kil 1* core retrieved from the NE part of the Kilia Promontory (Fig. 1) intercepted the pre-deltaic loess from 400 to 300 cm which is overlaid by poorly to medium sorted silts from 300 to 180 cm (Fig. 5).

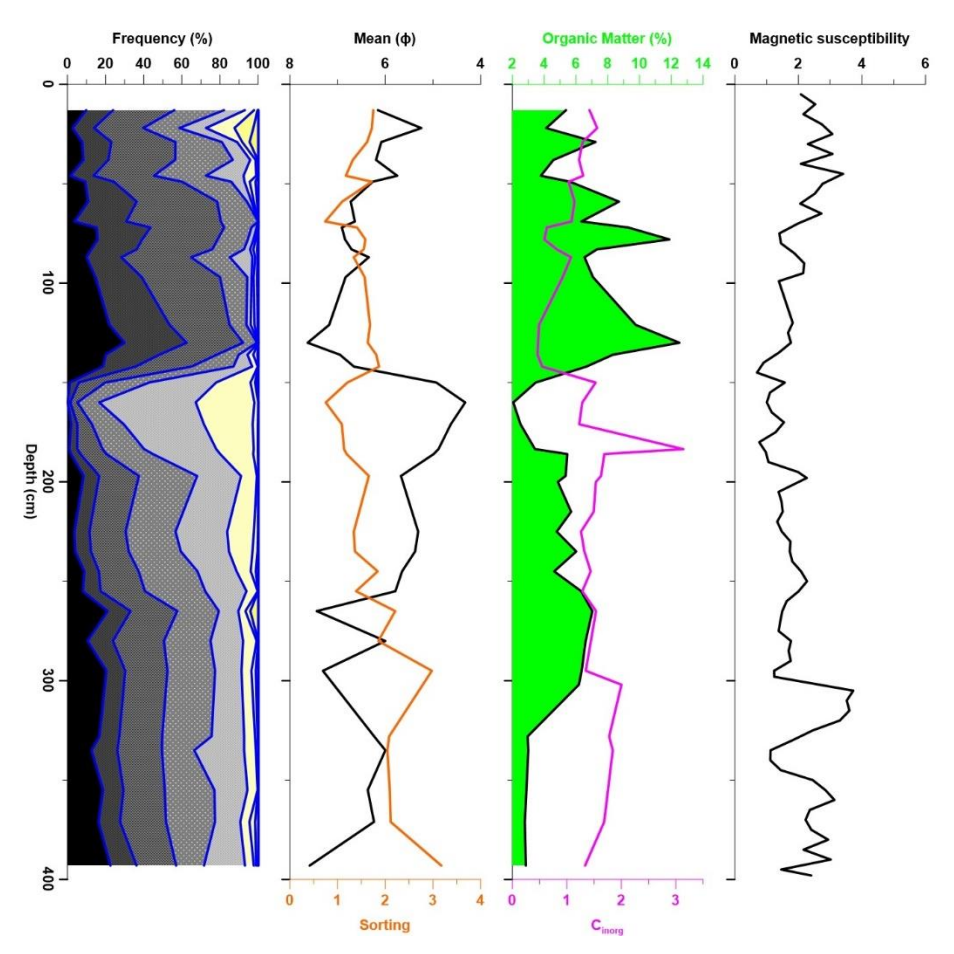


Figure 5 Grain size and sorting, organic matter content and magnetic susceptibility on Kil 1 core A sudden increase of the grain size is marked by well sorted gradual upcore coarsening input of coarse silts and fine sands. Sand size sediment accumulation abruptly ceased at 150 cm once with the installation of finer and poorly sorted sediments accumulation regime. The change of the sedimentation regime is also accompanied by the increase of Corg and Cinorg matter content which peaks to 5% at 130 and 75 cm.

3.2. Geochemical analysis

The elemental concentration measurement provides useful insight on the mineralogical content and sedimentary characteristics either as bulk concentration of specific elements as for example K and Si which are directly related to certain grain size classes, or various ratios between geochemical elements (e.g. Ca/Fe, Zr/Rb, Si/S, Ca/Sr) which might be indicative of sedimentation environment characteristics (e.g. energetic regime, physical and chemical features). K content is usually associated with the weight of the finest sediment fraction such as clays. Si concentration reflects the trends of coarser siliciclastic fraction as silt or sand. Mineralogical determinations on

Kil 1 core show the coincident variation of the K and Si concentrations in the lower part of the core from 195 to 400 cm and their antagonistic pattern upcore likely in relation with the change of the sediment source and the advent of a coarser, sand-size allochthonous sediment (195 to 150 cm) followed by a switch toward a finer sediment input at the top of the core. The sudden increase of the K concentration paralleled by the decrease of the Zr/Rb ratio in the upper part of the core from 140 cm upward might be related to a change toward finer and calmer depositional environment (Fig. 6).

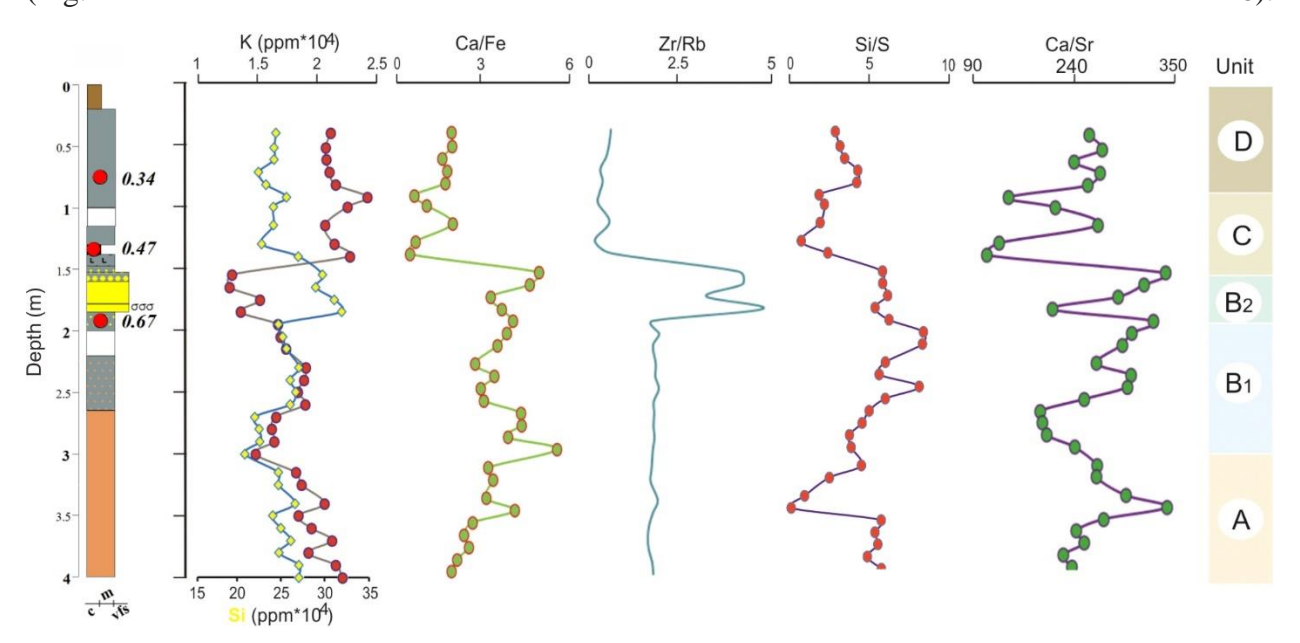


Figure 6 Geochemical profile on Kil core

The Zr/Rb ratio as erosional proxy ratio is particularly important as it highlights the succession of three different energetic environments: between 400... 185 cm, 185...150 cm and 150...0 cm. As such, the large values as between 180...150 cm indicates more energetic depositional conditions, in agreement with textural data which get coarser at this depth. Si/S ratio varies greatly along the core displaying large values in association with the sediment advection pulses as from 315 to 155 cm depth and lower values indicative of stagnant water regime as at 350 cm, 130 cm, 92 cm depth. A similar trend but with more ample fluctuations is depicted by the Ca/Sr ratio which is expected to account for the saline conditions (in relation with either marine water intrusion or dessication) as the low values (Ca/Sr: <50) of the ratio should correspond to higher salinity conditions, whereas the greater values (Ca/Sr: >290) such as at 240 cm, 195 and 155 cm should be related to freshwater advection pulses (cf. Hadler et al., 2018) (Fig. 6). The

Ca/Sr ratio profile at Kil 1 core location shows a sudden freshwater input at 350 cm after constant average values beneath this depth. This change of Ca/Sr ratio values is coeval with the stratigraphic change from loess to homogenous silts. This freshwater pulse is followed by a gradual upcore increase of salinity until 270 cm. From this depth upward several pulses of freshwater input can be distinguished at 240 cm, 195 cm, 155 cm. From 155 to 95 cm the fluctuations of Ca/Sr ratio might be influenced by carbonates content and further upcore by salinization processes specific to desiccated lands. However, the values from the last upper meter are comparable to those obtained in the lowermost half of meter where terrestrial loess has been intercepted.

Microfauna inventory

On KIL core, the first microfaunal evidence appears in the upper levels above the loess deposits (Annex 1). In the silty interval from 300 cm to 223 cm, microfauna is rare, as it is only found in a few specimens of foraminifera and brackish and freshwater ostracods. Starting at a depth of 180 cm to 152 cm, microfauna is much more abundant, represented by numerous specimens of euryhaline foraminifera *Ammonia beccari* and *Porosononion* sp., along with brackish ostracods such as *Tyrrhenocythere amnicola*, *Calistocythere diffusa*, *Amnicythere multipunctata*, *Amnicythere bendovanica*, *Loxoconcha* sp., *Candona schweyeri*, *Limnocythere inopinata*, and the euryhaline species *Cyprideis torosa*. There are also some freshwater ostracods, mainly *Darwinula stevensoni*, *Ilyocypris gibba*, *Ilyocypris bradyi*, *Eucypris dulciformis*, *Cypridopsis vidua*, *Pseudocandona compressa*, *Cypria ophtalmica*, *Candona neglecta*, and *Cyclocypris laevis*. From the 152m level in this core, the upper clay sediments no longer contain foraminifera and brackish ostracods. Only freshwater ostracod can be identified, particularly specimens of *I. gibba*, *I. bradyi*, *P. compressa*, and *C. neglecta* (*Annex 1*).

Palynological analysis

Spores-pollen analysis was undertaken on Kil1 core. No pollen grains were detected deeper than - 1.4m. Three main layers have been distinguished according to the variability of the pollen content (Annex 2):

LPAZ-C1 -high non-arboreal pollen (AP) values up to 73 % and highest trees value (27 %) in the profile. Herbaceous vegetation is represented by: *Poaceae*, *Chenopodiaceae* and *Aster type type* and *Artemisia and Apiaceae*.

Trees are represented mainly by *Quercus*; other deciduous broadleaved trees like *Betula*, *Ulmus* and *Tilia are* present but with low values. *Pinus* is also present but below 10% so long-distance transport should be considered.

Among the marsh and aquatics Cyperaceae are the most abundant (up to 40%).

LAPAZ-C2 -abrupt increase in microscopic charcoal concentrations (CHAC), indicating a strong fire episode in this zone with one major peak in subzone C-2a at about 0.4 cal. yr. BP followed by a decrease (yet still high) and a secondary much smaller peak in subzone C-2b at about 0.49 cal. yr. BP.

Subzone C-2a - decrease in trees (to 10%) when CHAC reaches maximum. Herbs continue to dominate. Decrease in *Poaceae* (15%) at 134 cm but will increase to 23% immediately after and will keep this value till C2-b. Consistent peak in *Chenopodiaceae* (28%) and *Aster type* (20%), immediately followed by a maximum peak in *Brassicaceae* reaching 28%. Also, minimum value of *Artemisia* and a small peak in Pinus (10 %). Small increase in *Rosaceae* and *Avena-Triticum type*. *Polygonum aviculare* increases shortly after max CHAC, towards top of subzone.

After the maximum CHAC peak, between subzones C-2a and C-2b (from 124 to 80 cm depth) trees have a small increase especially *Quercus* and also there is a small increase in *Artemisia*. *Salix* increases (but low) compared to C-1 but will reduce again towards top of the zone. *Brassicaceae* will have a second peak at 100 cm depth reaching 20 %, but will drastically reduce from now. Around 90 cm depth shrubs have a small increase represented by *Corylus* together with a small increase in *Betula*, *Ulmus* and *Alnus* and a decrease in *Quercus*. *Aster type* decreases signifyingly during this time span. *Juglans* peak around 120 cm depth, *Avena-Triticum type* and *Hordeum type* increase toward the upper part of this zone.

Subzone C-2b small increase in CHAC while tree and shrubs diminish. There is an abrupt increase in *Chenopodiaceae* together with an increase in *Aster type* and reductions in *Poa* and *Artemisia*. Also, there is a small increase in *Potamogeton* and *Nymphoides peltata*.

LAPAZ-C3- further decrease in CHAC except at 43 cm depth where it has a small peak. *Chenopodiaceae* remain high, they have a small decrease when CHAC decreases but will reach 60% and become the dominant herb in the top of the profile. *Quercus* again has a small increase when CHAC decreases and *Pinus* increases toward top in C-3a and C-3b b. Small increase in shrubs starting from 58 cm upwards. Trees decrease in C-3b reaching lowest value in profile of 16%, while *Corylus* increases. *Brassicaceae* have a very small increase at 43 cm depth. *Poaceae*

increase but then decrease reaching 10 % towards the top. *Aster type* decreases and finally disappears towards top. Increase in *Carpinus* especially *Carpinus orientalis* through the hole zone and *Betula* in the lower part, while *Corylus* has a small increase throughout the zone.

Juglans reappears but lower, Avena-Triticum type reappears in C-3a and C-3b. Hordeum type increases compared to C-2b and keeps constant. Centaurea nigra has a small increase in C-

3a and *Potamogeton* is present in C3 but very low and then further diminishes. *Zygnemataceae* appear in C-3b. *Cyperaceae* small increase but decrease to 10 % towards the top. The top unit (30 – 0 cm) has a lower charcoal concentration (1.6-5.5 particles/cm³) sourced from woods and herbaceaous material.

The newly obtained geo-scientific data were confronted with the archaeological evidence and historical information to track the pattern of navigable routes at different historical moments in the Danube delta. The envisaged scenarios are detailed one publication submitted to The Holocene (see publications list) (Annex 3)

Papers:

- Țuțuianu, L., Vespremeanu-Stroe A., Pendea, F., Sava, T., 2018. Mid and Late Holocene evolution of Brateș Lake region (Danube Floodplain) based on multiproxy analyses. Revista de Geomorfologie (2018)
- 2. Preoteasa, L. 2019. Morphological changes in the proximity of the Greek colonies founded along the western (Romanian) Black Sea coast: Orgame, Histria, Tomis, and Kallatis. *Revista de Geomorfologie* 21, 15-28.
- 3. Preoteasa, L., Vespremeanu-Stroe, A., Dan, A., Țuțuianu, L., Panaiotu, C., Stoica, M., Sava, T., Iancu, L., Stanică, A., Zăinescu, F., Mirea, D., Olteanu, D. Submis. Landscape evolution and human presence in the northern Danube delta (Chilia lobes) *The Holocene, submitted*.
- 4. Țuțuianu, L., Vespremeanu-Stroe, A., Preoteasa, L., Rotaru, S., Sava, T., Dimofte, D., accepted for publication. Wetlands and Lakes Formation and Evolution on the Lower Danube Floodplain during Mid and Late Holocene, *Quaternary International*.
- 5. Preoteasa, L., Hanganu, D., Vespremeanu-Stroe, A., Dan, A., Florescu, G, Sava, G., Pascal, D., Olteanu, D, Stănică, A., Paleoecological data and historical evidence document Chilia foundation and its role in social economic activity at the mouths of the Danube in the Medieval Ages, *Journal of Archaeological Science*, *submitted*

PhD Thesis

Ţuţuianu, L., Holocene evolution of the Lower Danube Valley between Brăila and Ceatal Izmail (2021)

Zăinescu, F., Fluvio-marine interaction and sediment dynamics in river mouth areas (2019)